Proceedings of the 4th International Topical Meeting on High Temperature Reactor Technology
HTR2008
September 28-October 1, 2008, Washington, DC USA

HTR2008-58281

CREEP EFFECTS ON DESIGN BELOW THE TEMPERATURE LIMITS OF ASME SECTION III SUBSECTION NB*

T.-L. (Sam) Sham
Oak Ridge National Laboratory
Oak Ridge, Tennessee, USA
Email: shamt@ORNL.gov

Robert I. Jetter
Consultant
Pebble Beach, California, USA

Daniel R. Eno
Consultant
Guilderland, New York, USA

ABSTRACT

Some recent studies of material response have identified an issue that crosses over and blurs the boundary between ASME Boiler and Pressure Vessel Code Section III Subsection NB and Subsection NH. For very long design lives, the effects of creep show up at lower and lower temperature as the design life increases. Although true for the temperature at which the allowable stress is governed by creep properties, the effect is more apparent, e.g. creep effects show up sooner, at local structural discontinuities and peak thermal stress locations. This is because creep is a function of time, temperature and stress and the higher the localized stress, the lower in temperature creep begins to cause damage. If the threshold is below the Subsection NB to NH temperature boundary, 700ºF for ferritic steels and 800ºF for austenitic materials, then this potential failure mode will not be considered.

Unfortunately, there is no experience base with very long lives at temperatures close to but under the Subsection NB to NH boundary to draw upon. This issue is of particular interest in the application of Subsection NB rules of construction to some High Temperature Gas Reactor (HTGR) concepts.

* Notice: This submission was sponsored by a contractor of the United States Government under contract DE-AC05-00OR22725 with the United States Department of Energy. The United States Government retains, and the publisher, by accepting this submission for publication, acknowledges that the United States Government retains, a nonexclusive, paid-up, irrevocable, worldwide license to publish or reproduce the published form of this submission, or allow others to do so, for United States Government purposes.

The purpose of this paper is, thus, twofold; one part is about statistical treatment and extrapolation of sparse data for a specific material of interest, A533B**;** the other part is about how these results could impact current design procedures in Subsection NB.

Introduction

The ASME Boiler and Pressure Vessel (B&PV) Code, Section III, Subsection NB provides construct rules for Class 1 nuclear components. The Subsection NB code materials and their corresponding primary stress limits are tabulated in Section II, Part D, Tables 2A (ferrous materials) and 2B (nonferrous materials). Table 4 of Part D gives the stress limits for bolting materials. The Subsection NB rules shall not be used for materials at design temperatures that exceed the maximum temperature limits listed in the applicability columns of these tables. They are 700°F for ferritic steels and 800°F for austenitic steels. For temperatures above these limits the rules of construction for Class 1 nuclear components are provided in Section III, Subsection NH, but the number of approved Subsection NH code materials is much more limited.

Current view among many concerning Code boundary of Subsections NB and NH is that creep effects do not need to be considered for temperatures below 700ºF for ferritic steels in reactor pressure vessel (RPV) applications. While this is undoubtedly true for typical Light Water Reactor operating temperatures, it may not be true for higher normal operating metal temperatures

 Copyright © 2008 by ASME

that are pushing against the 700ºF boundary, e.g., at 660ºF, and for a long design life, e.g., 60 years. This is particularly poignant with the consideration of localized high stress areas. The reason is that creep deformation depends on stress, time and temperature and does not have a strict temperature cut-off that separates creep from non-creep regimes. This could potentially affect the primary stress limits and impact RPV sizing. The potential impact could also likely show up at structural or metallurgical discontinuities. If there is a real problem in the RPV due to creep effects at 660ºF it is not likely to show up until the component is well into its operating life.

Creep data at these low temperatures are very difficult to develop as it is not practical to perform creep tests for such long durations. Accelerated tests would in general be relied upon to generate data for extrapolation. The only currently available data that could provide limited information in framing the issue of whether or not the consideration of creep is needed for the RPV in the upper temperature limit of Subsection NB for very long design lives are those that supported the development of Code Case N-499, which provides rules of construction for two specific low-alloy steels: A533B (UNS K12539) plates and A508 Class 3 forgings (UNS K12042) and their weldments for short-term temperature excursions above the temperature limit of 700°F.

A533B Database

The creep database (McCoy, 1990) that supported Code Case N-499 was a subset of the data reported by McCoy (1989). It consisted of 50 creep rupture test results from four A533B plate heats. The applied stresses ranged from 1 to 75 ksi, and the test temperatures ranged from 700°F to 1100°F. Of the 50 test results, 15 tests were reported to have terminated in creep rupture, and 35 tests were reported to have terminated prior to the occurrence of creep rupture. All four heats were represented in each group of results. Test data included time to 1% strain ($t_{1\%}$), time to start of tertiary creep ($t_{tertiary}$), and time to creep rupture (t_r), where applicable. The longest creep rupture time was 3,378 hours and the shortest was 23.5 hours. The longest test time where the test was terminated before creep rupture took place was 25,921 hours and the shortest was 285 hours.

As the objective of Code Case N-499 was to develop time dependent primary stress limits for limited numbers of short-term elevated temperature excursions, only the tests that resulted in creep rupture were analyzed during the development of the code case. However, the results from those tests that were terminated before creep rupture occurred do provide valuable information on the creep rupture behavior at longer exposure times. This can be accomplished by treating these results as censored data and to estimate the model parameters using maximum likelihood estimation. The strategy is then to use the results from the entire A533B database to develop a statistical model, and to extrapolate the resulting statistical model to conditions that are of interest to addressing the effects of creep at lower temperatures and longer exposure times. However, it should be recognized that extrapolation far away from the test conditions of a database might not always be reliable; hence, one should be mindful of this in assessing the extrapolated results. Nevertheless, in the absence of data that are more representative of the conditions of interest, the results presented herein provide the first opportunity to explore this difficult subject.

Statistical Methods

Following Eno et al. (2008), each of the three time responses was analyzed via regression modeling as a function of applied stress (σ, ksi) and temperature (T, °F), using the following linear model forms:

$$\ell n(t) = \beta_0 + \frac{\beta_1}{T_R} + \beta_2 \ell n(\sigma) + \frac{\beta_3}{T_R} \ell n(\sigma) \qquad (1)$$

$$\ell n(t) = \beta_0 + \beta_1 T_R + \beta_2 \ell n(\sigma) + \beta_3 T_R \ell n(\sigma) \qquad (2)$$

where $T_R = T + 460$ is the absolute temperature in Rankine. The parameters β_0, β_1, β_2 and β_3 were estimated using several common creep parameterizations, all of which are special (in some cases constrained) cases of equations (1) and (2):

- Mendelson-Roberts-Manson (MRM) uses equation (1) (no parameters fixed at zero);
- Orr-Sherby-Dorn uses equation (1), with the parameter β_3 fixed at zero;
- Larson-Miller uses equation (1), with the parameter β_2 fixed at zero;
- Manson-Haferd uses equation (2) (no parameters fixed at zero);

 Copyright © 2008 by ASME

- Manson-Succop uses equation (2), with the parameter β_3 fixed at zero.

Statistical Results

The five regression model formulations described above were fit to each of the three responses ($t_{1\%}$, $t_{tertiary}$, t_r) via the method of maximum likelihood estimation. A log-normal distribution was assumed for each response variable's random error distribution. Table 1 summarizes the optimized value of negative two log-likelihood (–2LL) for each model and each response. For two nested models (that is, two models for which one represents a restriction of the other), a statistical test for the adequacy of the simpler (restricted) model can be performed based on the difference in –2LL between the two fitted models. This difference will have an asymptotic chi-squared distribution, with degrees of freedom equal to the difference in number of parameters between the two nested models.

Table 1. Negative two-log-likelihood values

Model	–2LL for $t_{1\%}$	–2LL for $t_{tertiary}$	–2LL for t_r
MRM	126.45	115.64	71.50
Orr-Sherby-Dorn	167.94	133.12	88.30
Larson-Miller	164.87	130.91	86.52
Manson-Haferd	132.29	116.96	71.73
Manson-Succop	164.76	129.38	86.08
Mean Only	181.09	146.29	96.07

From Table 1, it can be observed that the restricted version of equations (1) and (2) (namely, Orr-Sherby-Dorn, Larson-Miller, and Manson-Succop) provide significantly inferior fits than the unrestricted versions (MRM and Manson-Haferd). There is a slight preference for the MRM model over the Manson-Haferd model for each of the three responses, on the basis of the optimized –2LL values. Therefore, subsequent calculations will be based on the MRM model.

Also included in the last row of Table 1 are the –2LL values for simple "mean only" models for the three responses; these models assume no dependence of the response on applied stress or temperature. Based on comparing these –2LL values with the values for the MRM model, it can be seen that the overall dependence of each response on the predictors (stress and temperature) is statistically significant.

For a ruptured specimen, the time to the start of tertiary creep is necessarily shorter than the rupture time. However, when the regression results are extrapolated far away from the database, it is possible that the extrapolated value of $t_{tertiary}$ could be larger than that of t_r when the regressions for the response times are performed independently. In order to prevent such an undesirable feature and yet to be able to explore the effects of creep at low temperatures and longer exposure times, the results to be reported in the following sections were obtained by assuming that each of the regression variables, β_1, β_2 and β_3, has the same value for all three response times, while the variable β_0 has different value for each response time.

Table 2 displays the estimated parameters for the MRM models, for the three response variables. The parameter γ is the estimated residual standard deviation, quantifying "data scatter" in the natural logarithm time space.

Table 2. Parameter Estimates for the MRM Model.

	$t_{1\%}$	$t_{tertiary}$	t_r
β_0	–1.394312E+02	–1.379852E+02	–1.366732E+02
β_1	2.350708E+05	2.350708E+05	2.350708E+05
β_2	2.598133E+01	2.598133E+01	2.598133E+01
β_3	–4.578777E+04	–4.578777E+04	–4.578777E+04
γ	9.926518E-01	1.222379E+00	1.435087E+00

Equation (1) for the MRM model can be recast in the form

$$t = A \ \exp\left(\frac{Q}{R\,T_R}\right)\sigma^{m(T_R)} \tag{3}$$

where $A \equiv \exp(\beta_0)$, $Q \equiv R\,\beta_1$, $m \equiv \beta_2 + \beta_3/T_R$, and R the Universal Gas constant. Note that $Q > 0$ and $m < 0$.

Copyright © 2008 by ASME

Figure 1. Measured versus predicted time to 1% strain

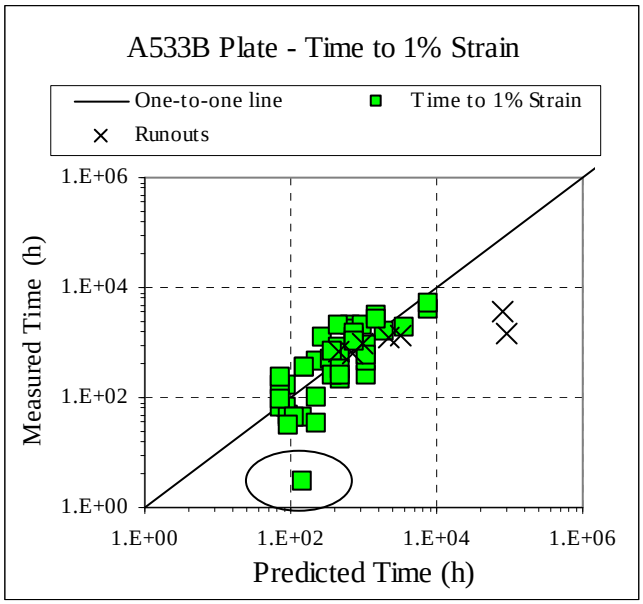

Figure 2. Measured versus predicted time to start of tertiary creep

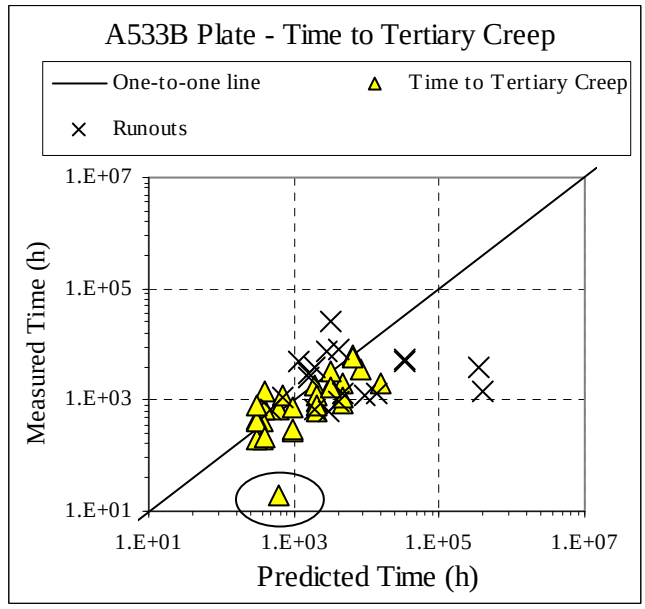

Figure 3. Measured versus predicted creep rupture time

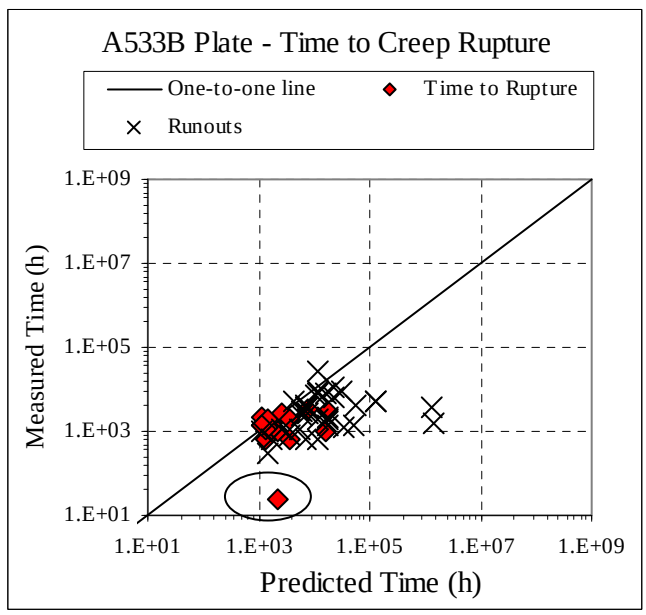

Figures 1 to 3 display the measured times from the database versus the predicted times from the MRM model. The solid symbols represent exact (uncensored) times; the crosses represent right censored times. In interpreting these plots, a tight fit to the database should have the exact times falling near the identity (one-to-one) line, and the crosses should tend to fall below the identity line. Of course, data scatter will also be exhibited by the data, so these tendencies will not be perfect, even for a good fit. Also, a large fraction of right censored data points (e.g., for the rupture time fit) will tend to push the prediction line higher; this is appropriate, since the right censored points tend to exhibit resistance to reaching the response criterion (e.g., rupture).

The results shown in Figure 3 can also be viewed from a different perspective. The region below the one-to-one line is where the actual time is shorter than the predicted time. If the tests of all the 50 specimens were carried out till rupture, it would be expected that somewhere around 25 data point are below the line, and 25 above the line. However, there are only 10 rupture data below the line in the figure, with many of the "survivors" below the one-to-one line, and had the tests been continued to rupture, some of them would have ruptured below, and some above, the one-to-one line.

From Figures 1 to 3, a single low outlier (the low measured time) is evident in all three plots. The outlier (circled) in all three plots corresponds to the same specimen.

Confidence and prediction bounds for times to 1% strain, start of tertiary creep, and rupture can be made from the MRM fits, based on equation (1) and the

Copyright © 2008 by ASME

coefficient estimates in Table 2. The q quantile confidence bound of $\ell n(t)$ can be estimated as

$$CB[\ell n(t)]_q = \{x\}^t \cdot \{\beta\} + z_q \cdot (se)_q \tag{4}$$

where

$$\{x\}^t = \lfloor 1,\ T_R^{-1},\ \ell n(\sigma),\ T_R^{-1}\ell n(\sigma) \rfloor \tag{5}$$

$$\{\beta\}^t = \lfloor \beta_0,\ \beta_1,\ \beta_2,\ \beta_3 \rfloor \tag{6}$$

with z_q represents the q quantile of the standard normal distribution, and $(se)_q$ is the standard error of a predicted quantile of $\ell n(t)$, at specified absolute temperature T_R, stress σ, and q quantile. For example, the 0.05 and the 0.95 quantiles are computed with using $z_{0.05} = -1.645$ and $z_{0.95} = +1.645$ in equation (4), respectively.

The standard error, $(se)_q$, can be computed as

$$(se)_q = \sqrt{\{y_q\}^t \cdot [V] \cdot \{y_q\}} \tag{7}$$

where

$$\{y_q\}^t = \lfloor 1,\ T_R^{-1},\ \ell n(\sigma),\ T_R^{-1}\ell n(\sigma),\ z_q \rfloor \tag{8}$$

and $[V]$ is the covariance matrix of the parameter estimate vector $\{\mu\}$, with

$$\{\mu\}^t = \lfloor \beta_0,\ \beta_1,\ \beta_2,\ \beta_3,\ \gamma \rfloor \tag{9}$$

where γ is the residual standard deviation estimate. Covariance matrices estimated from the fitted models for the three fitted models are given in the Appendix. The percentile prediction bound of $\ell n(t)$ can be estimated as

$$PB[\ell n(t)]_q = \{y_q\}^t \cdot \{\mu\} + z_q \cdot (se)_q \tag{10}$$

Since the response variable in a creep experiment is *time*, the predicted quantiles are appropriately expressed in terms of time for fixed stress and temperature (cf., equations (4) and (10)). If a bound on stress is desired, for fixed temperature and time, this can be obtained by algebraic rearrangement of the prediction equation for $\ell n(t)$. However, since the prediction standard error is a function of stress, this algebraic equation will in practice require numerical solution. For example, for a fixed temperature T_R, a given time t_0, and a prescribed q quantile, the corresponding stress σ can be computed from equation (10) numerically.

Figure 4 shows the examples of extrapolated creep rupture stress curves from the regression results as a function of time at 644ºF, 662ºF and 700ºF.

Figure 4. Extrapolated minimum creep rupture stress

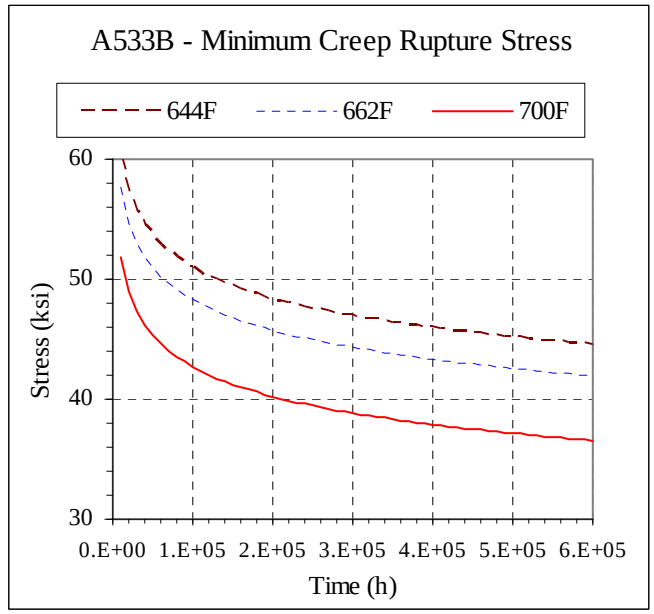

Time-Dependent Primary Stress Limit

Based on extrapolations in time up to 600,000 hours and in the temperature range of 644ºF to 750ºF, the values of the time-dependent primary stress limit, S_t, were established, following the Subsection NH procedure, as the smaller of

- 100% of average stress required to obtain a total strain of 1%;
- 80% of the minimum stress to cause initiation of tertiary creep; and
- 67% of the minimum stress to cause rupture

A quantile value of $q = 0.05$ was used in the prediction bounds to determine the minimum stresses in the above criteria. The values of S_t as a function of temperature at 100,000 hours, 300,000 hours, and 600,000 hours are shown in Figure 5. Figure 6 shows the S_t values as a function of time at 644ºF, 662ºF and 700ºF. The criterion that controls the S_t values for the conditions considered in these figures is two-thirds of minimum rupture stress. The time-independent primary stress limit, S_m, is also shown in these two figures for comparison.

Copyright © 2008 by ASME

Figure 5. Extrapolated time-dependent primary stress limits around the NB/NH temperature boundary

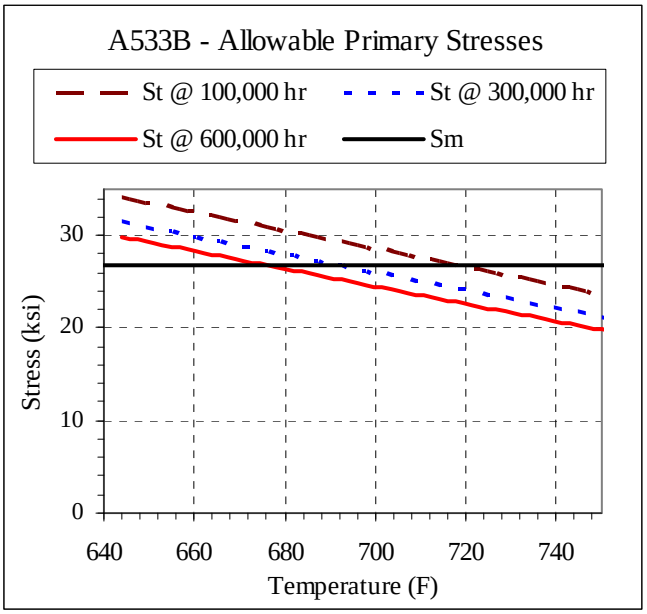

Figure 6. Extrapolated time-dependent primary stress limits as a function of time

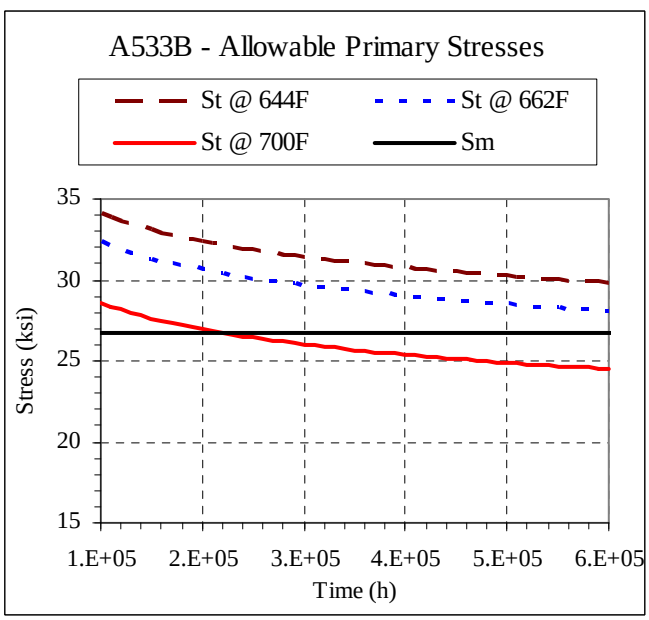

It should be noted that sizing methods in Subsections NB and NH are somewhat different. In Subsection NB, the wall thickness is sized based on the design condition while both design condition (based on 100,000-hour allowables as in Section VIII) and operating conditions are used in Subsection NH. Further, the limit in Subsection NB on P_m is S_m and on $P_L + P_b$ is $1.5S_m$, while in Subsection NH the limit on P_m is S_{mt}, on $P_L + P_b$ is $1.5S_m$, and in addition, the limit on $P_L + (P_b/1.25)$ is S_t. Since the Subsection NH limit of S_{mt} is the lesser of S_m and S_t, the limits on the general membrane stress intensity P_m from Subsections NB and NH can be compared by considering the relative magnitudes of S_m and S_t.

The extrapolated results in Figures 5 and 6 show that the time-independent primary stress limit S_m is lower, and hence conservative, than the time-dependent primary stress limit S_t for times up to 600,000 hours at 644ºF and 662ºF. At the Subsection NB cut-off temperature of 700ºF, S_m is non-conservative for lifetimes beyond approximately 220,000 hours.

The preceding discussion relates to effect of creep on the primary stress limit; however, the effects of creep will show up at a lower temperature at local structural discontinuities and peak thermal stress locations where the local stress is higher than the primary membrane stresses. In Subsection NH, these peak stress locations are considered in establishing negligible creep criteria above which time and temperature the effects of creep must be considered with explicit evaluation procedures. These criteria are based on the idea that the localized peak stress will be limited by the flow strength of the material.

One of the negligible creep criteria in Subsection NH, article T-1324 is

$$\sum_i \frac{t_i}{t_{id}} \leq 0.1 \tag{11}$$

where t_i is total duration of time during the service lifetime that the metal is at temperature T_i, and t_{id} is the rupture time given by the minimum rupture stress that is equal to $S_y)_{T_i}$, the minimum monotonic yield strength at temperature T_i, times a factor s which is equal to 1.5. The factor s is based on a factor of 1.25 to bring the minimum monotonic yield strength at temperature to the average value, and a factor of 1.2 to account for cyclic hardening of austenitic stainless steel in order to approximate the achievable stress state at geometric discontinuities. The appropriate value of s for ferritic steels such as A533B is not known.

Copyright © 2008 by ASME

The negligible creep time-temperature curves for selected values of the factor s can be obtained by using the yield strength at temperature from Table Y-1 of Section II Part D, the rupture time from equation (10) with $q = 0.05$, and the negligible creep criterion of equation (11) using the equality sign. These curves are shown in Figure 7.

Figure 7. Negligible creep curves

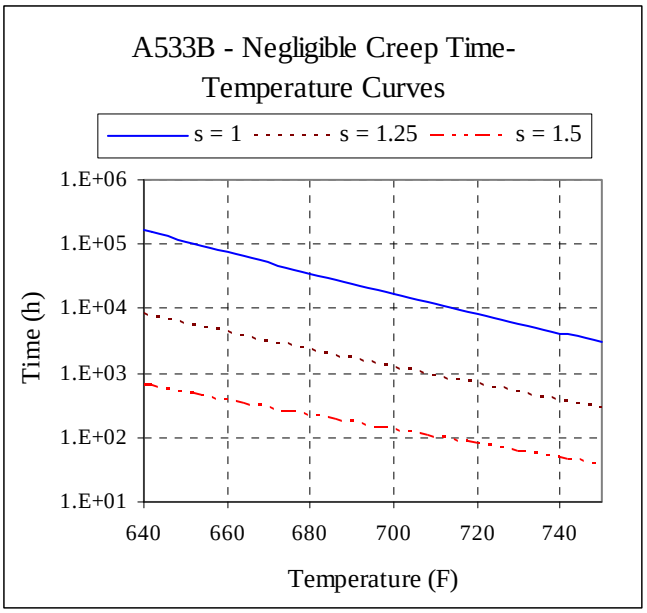

As can be seen from the plots in Figure 7, the use of $s = 1.5$ per article T-1324 of Subsection NH is very limiting and Code efforts to reassess the appropriate value to be used as the minimum creep rupture stress in determining the rupture time in equation (11) are needed. It is also noted that the factor 0.1 on the right hand side of equation (11) is applicable to all materials, per article T-1324 of Subsection NH. However, the negligible creep criteria are developed based on the assessment of the impact of creep damage on the fatigue performance. Since the creep-fatigue interaction as captured by the creep-fatigue interaction diagram of Subsection NH Appendix T is material specific, the factor on the right hand side of equation (11) should account for the differences in creep-fatigue behavior of different materials, e.g., the difference in the "knee' of the creep-fatigue interaction diagram.

Discussion

To put the results that were presented in Figures 4 to 6 into perspective, it is well to recognize that the extrapolations are based on a small database with relatively short-term creep data as compared with the extrapolated times of 500,000 to 600,000 hours. Thus definitive conclusions could not be drawn based on these results. However, the results shown in these figures do underscore the need to develop longer term confirmatory creep rupture data, and to follow-up on the creep-fatigue issue to ensure that creep effects are properly accounted for in design for very long operating lives.

Creep-rupture and fatigue damage are the areas that need particular attention for A508 Class 3 and A533B steels and their associated weldments to assess the current temperature boundary between Subsections NB and NH. These areas requiring attention are closely related to the definition of when creep effects become significant. Simplified bounds for creep ratcheting, strain and deformation limits, and use of simplified rules to bound stress concentrations are related issues that also need to be considered. To address these issues, it is important to understand how ratcheting, strain limits and creep fatigue affect the integrity of a structure differently.

Creep-fatigue is a localized issue whereas ratcheting is based, conceptually, on the interaction of the core stress and linearized through-wall stress (in the Bree model). Also, creep-fatigue is a direct failure mode whereas ratcheting is not. Cyclic life can, conceptually, be influenced directly by creep rupture damage at lower temperature whereas ratcheting would most likely be influenced by degraded tensile properties due to aging, or, potentially, cyclic softening, either from long term exposure at normal operation and/or short term, higher temperatures. Within the negligible creep regime, Subsection NH relies on $3\bar{S}_m$ where the limit is based on the relaxation strength to ensure shakedown.

Test data are needed to address creep rupture and creep-fatigue, and the issues of whether or not the material properties at normal operating temperatures are compromised by short term, higher temperature off normal conditions. Data on the relaxation strength under these conditions will also be helpful in addressing the issue. Due to a lack of operational experience in using A508 Class 3 and A533B pressure vessel steels at these high temperatures for very long times, confirmatory data on thermal aging, environmental effect, and neutron

Copyright © 2008 by ASME

irradiation embrittlement are needed to also assess their impact on the Code transition temperature.

Summary

The A533B creep data that supported Code Case N-499 were analyzed using statistical models. The regression results were extrapolated to very long times, up to 600,000 hours, in order to explore the effects of creep on long design lives and at metal temperatures that are below the Subsection NB limit of 700ºF.

Based on the extrapolated results, it was found that RPV sizing based on Subsection NB rules might not be conservative, and one of the negligible creep criteria of Subsection NH could not be satisfied, for designs with long design lifetimes and at metal temperatures that are within the limit of Subsection NB. This suggests that design for creep-fatigue interaction might be necessary towards the later part of the operating life of the RPV. Code efforts to reassess the negligible creep criteria are recommended.

These concerns notwithstanding, it is well to recognize that these observations were based on the extrapolation of a very small database, with relatively short creep times, to conditions that are very far away from those employed in the tests. Thus definitive conclusions could not be drawn based on these results. However, the results presented in this paper do underscore the potential problems of an artificial temperature boundary between Subsections NB and NH, particularly with future HTGR components that have very long lifetimes and metal temperatures that push against this boundary. Hence Code development efforts are sorely needed in order to push the HTGR technology forward.

References

Eno, D.R., Young, G.A., and Sham, T.-L., “A Unified View of Engineering Creep Parameters,” ASME PVP2008-61129, 2008.

McCoy, H.E. “Tensile and Creep Properties of SA533 Grade B Class 1 Steel,” Report No. ORNL/TM-11338, ORNL, Oak Ridge, TN, USA, December, 1989.

McCoy, H.E., Data Package submittal to ASME B&PVC SG-ETC, SC II SG-SFA, and SG-ETD, April 17, 1990.

Copyright © 2008 by ASME

Appendix

Covariance Matrix $[V]$ for different response times:

	$t_{1\%}$				
	β_0	β_1	β_2	β_3	γ
β_0	2.492387E+02	–3.965339E+05	–4.801997E+01	8.110106E+04	0.000000E+00
β_1	–3.965339E+05	6.315536E+08	7.604371E+04	–1.287563E+08	0.000000E+00
β_2	–4.801997E+01	7.604371E+04	9.581778E+00	–1.594818E+04	0.000000E+00
β_3	8.110106E+04	–1.287563E+08	–1.594818E+04	2.672820E+07	0.000000E+00
γ	0.000000E+00	0.000000E+00	0.000000E+00	0.000000E+00	1.137413E-02
	$t_{tertiary}$				
	β_0	β_1	β_2	β_3	γ
β_0	2.487363E+02	–3.961219E+05	–4.797869E+01	8.102603E+04	0.000000E+00
β_1	–3.961219E+05	6.315536E+08	7.604371E+04	–1.287563E+08	0.000000E+00
β_2	–4.797869E+01	7.604371E+04	9.581778E+00	–1.594818E+04	0.000000E+00
β_3	8.102603E+04	–1.287563E+08	–1.594818E+04	2.672820E+07	0.000000E+00
γ	0.000000E+00	0.000000E+00	0.000000E+00	0.000000E+00	2.494689E-02
	t_r				
	β_0	β_1	β_2	β_3	γ
β_0	2.477154E+02	–3.952839E+05	–4.787905E+01	8.085488E+04	0.000000E+00
β_1	–3.952839E+05	6.315536E+08	7.604371E+04	–1.287563E+08	0.000000E+00
β_2	–4.787905E+01	7.604371E+04	9.581778E+00	–1.594818E+04	0.000000E+00
β_3	8.085488E+04	–1.287563E+08	–1.594818E+04	2.672820E+07	0.000000E+00
γ	0.000000E+00	0.000000E+00	0.000000E+00	0.000000E+00	6.490728E-02

Copyright © 2008 by ASME